

Entropy and Earthward Transport in the Plasma Sheet

R. A. Wolf
Rice University

(Thanks to Colby Lemon and Jichun Zhang for use of
unpublished results)

Outline

1. Introduction/Outline
2. Basic Theory of Plasma-Sheet Entropy
3. Interchange Instability
4. Statistical Plasma-Sheet Models and Pressure Balance Inconsistency
5. Entropy-Conserving Self-Consistent Simulations
6. Bubbles in the Plasma Sheet and Creation Mechanisms
7. Restriction on Bubbles That can Reach the Inner Magnetosphere
8. RCM Simulation of a Bubble in a Substorm
9. RCM-E Simulation of Interchange Instability in a Sawtooth Event
10. Summary

2. Basic Theory of Plasma Sheet Entropy

Drift Motion on Closed Field Lines With Slow Flow

- Assume that the energy in drift motion is small compared to thermal energy (bounce and gyro motion), which allows use of the bounce-averaged-drift approximation.
- It is elegant to use Euler potentials ($\mathbf{B}=\nabla\alpha\times\nabla\beta$) to label the field lines and the drift motion of the particles [*Stern, Am.J.Phys.*, 38, 494, 1970], in which case the bounce-averaged-drift equations become simply

$$\frac{d\alpha}{dt} = \frac{1}{q} \frac{\partial H}{\partial \beta}, \quad \frac{d\beta}{dt} = -\frac{1}{q} \frac{\partial H}{\partial \alpha} \quad (1)$$

- These equations are equivalent to the equations for incompressible fluid flow in 2D. ($H\rightarrow$ stream function).
- Different useful approximations can be obtained by using different types of expressions for H .

Kinetic Theory Definition of Entropy

- Definition of entropy:

$$S = -\int d^3x \int d^3p f \ln(f) = -H_B V \quad (2)$$

where

$$N = \int d^3x \int d^3p f \quad (3)$$

H_B = Boltzmann H function, and f = distribution function (e.g., *Liboff, Kinetic Theory*, Sect. 3.3.7).

- If the particle motion is Hamiltonian, then f is conserved along a path in phase space, and the volume of phase space occupied by a set of particles on nearby trajectories is also conserved.
- If particle motion is determined by large-scale \mathbf{E} and \mathbf{B} , then the motion is Hamiltonian.
 - Collisional and dissipational processes typically make the motion non-Hamiltonian.

Entropy of a Perfect Gas

$$S = -\int d^3x \int d^3p f \ln(f) \quad (2)$$

$$N = \int d^3x \int d^3p f \quad (3)$$

- Isotropic perfect gas:

$$f = \frac{n}{W_o^{3/2}} g\left(\frac{W}{W_o}\right) \quad (4)$$

where n =number density, W =particle energy, n =number density, W_o =average energy, g = arbitrary function. Substituting (4) in (2) and (3) and using perfect gas law gives, for the entropy per particle

$$\frac{S}{N} = \frac{3}{2} \ln\left(\frac{P}{n^{5/3}}\right) + \Lambda \quad (5)$$

where Λ depends just on the shape of the distribution function.

- For Hamiltonian drifts, $P/n^{5/3}$ is conserved, provided that the volume of phase space occupied by the gas remains compact, so that you can relate what happens at (x, t) to what happened at (x', t') .

Plasma With Isotropic Pressure and Frozen-in Flux

$$\frac{S}{N} = \frac{3}{2} \ln \left(\frac{P}{n^{5/3}} \right) + \Lambda \quad (5)$$

- The easiest way to ensure that the distribution function remains compact is to take a Hamiltonian of the form

$$H = q\Phi(\alpha, \beta, t) \quad (6)$$

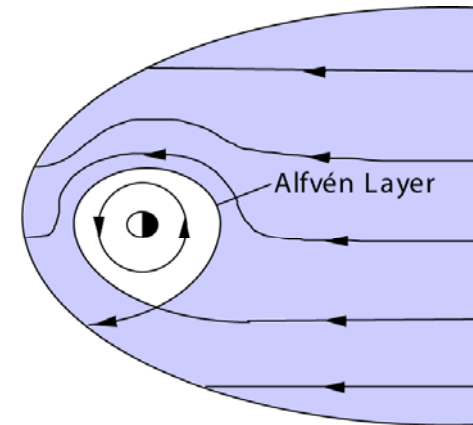
- Then the particle motion is $\mathbf{E} \times \mathbf{B}$ drift and $E_{\parallel} = 0$. That ensures frozen-in flux, which ensures the conservation of $N = nV =$ particles per unit magnetic flux, where $n =$ number density, and $V = \int ds/B$ is the volume of a tube of unit flux.

$$\frac{S}{N} = \frac{3}{2} \ln(PV^{5/3}) - \frac{5}{2} \ln(N) + \Lambda \quad (7)$$

- Thus Hamiltonian motion implies conservation of $PV^{5/3}$ along a drift path assuming isotropic pressure, frozen-in flux, no loss of particles from the flux tube, and also that the shape of the distribution function remains constant.

Application to the Magnetosphere

- Shaded region is one in which the flow is slow compared to MHD waves speeds.
- Ideal MHD case:
 - If $PV^{5/3}$ is uniform on the portions of the outer boundary where there is inflow, and independent of time, then $PV^{5/3}$ is uniform throughout the slow-flow region, except for the trapped-particle region.



Plasma With Isotropic Pressure and Particles That Gradient/Curvature Drift in Addition to ExB Drift

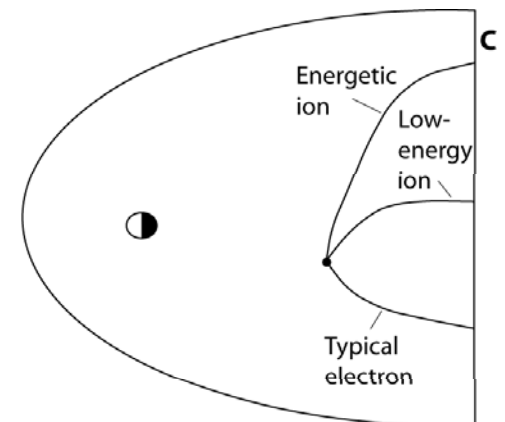
$$\frac{d\alpha}{dt} = \frac{1}{q} \frac{\partial H}{\partial \beta}, \quad \frac{d\beta}{dt} = -\frac{1}{q} \frac{\partial H}{\partial \alpha} \quad (1)$$

- The corresponding Hamiltonian is

$$H = q\Phi(\alpha, \beta, t) + \lambda V(\alpha, \beta, t)^{-2/3} \quad (8)$$

where λ = energy invariant. Substituting (8) in the drift equations (1) gives the standard equations for bounce-averaged ExB and gradient-curvature drift (e.g., *Harel et al., JGR, 86, 2217, 1981*) for isotropic pressure.

- Since now different particles drift at different velocities, the full region of phase space occupied by the plasma doesn't remain compact as the particles drift.
- The full S/N of the plasma is not conserved.
- It is useful to consider different regions of phase space separately.

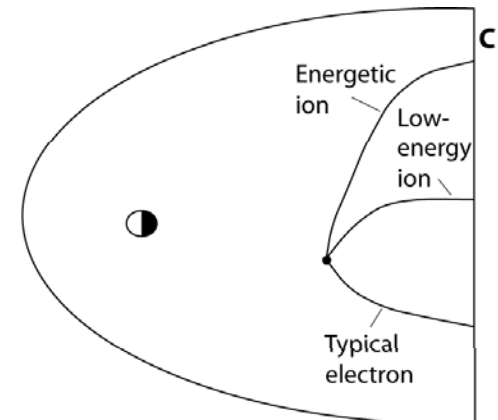


Plasma With Isotropic Pressure and Particles That Gradient/Curvature Drift in Addition to ExB Drift

- Divide the energy distribution up by chemical species and λ levels. Within each level $PV^{5/3}$ is conserved :

$$P(\mathbf{x},t)V(\mathbf{x},t)^{5/3} = \sum_s P_s[\mathbf{x}_{Cs}(\mathbf{x},t),t_{Cs}(\mathbf{x},t)]V[\mathbf{x}_{Cs}(\mathbf{x},t),t_{Cs}(\mathbf{x},t)]^{5/3} \quad (9)$$

- If the distribution function is uniform on the portion of the boundary where particles are entering the region, $PV^{5/3}$ is uniform throughout the sheet.
 - Except for the contribution of particles that are on trapped orbits.



Plasma Consisting of Particles That Drift Conserving First Two Adiabatic Invariants

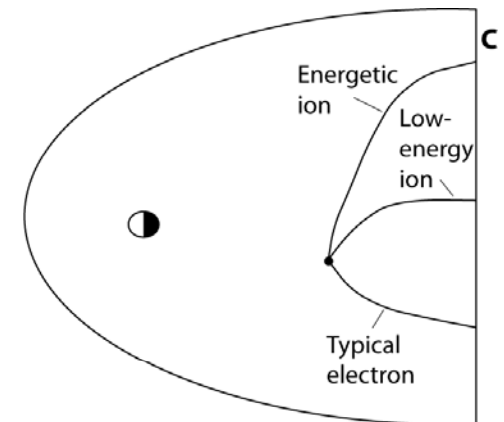
$$\frac{d\alpha}{dt} = \frac{1}{q} \frac{\partial H}{\partial \beta}, \quad \frac{d\beta}{dt} = -\frac{1}{q} \frac{\partial H}{\partial \alpha} \quad (1)$$

- The corresponding bounce-averaged-drift Hamiltonian is

$$H = q\Phi(\alpha, \beta, t) + W_K(\mu, J, \alpha, \beta, t) \quad (10)$$

where W_K is the kinetic energy in the particle's bounce and gyro motion, which usually has to be calculated numerically.

- Since this drift motion is Hamiltonian, f should again be conserved along a drift path.
- Entropy is still defined and conserved, but it isn't simply related to pressure or energy density.
- If we still use $PV^{5/3}$ conservation to estimate the total particle energy on a flux tube, do we underestimate or overestimate the adiabatic energization that accompanies earthward transport?
 - Answer: We underestimate it [Wolf *et al.*, *JGR*, 104, A00D05, 2009].



Concluding Comment on Entropy

- I will probably sometimes refer to $PV^{5/3}$ as “entropy”, but remember that

$$\frac{S}{N} = \frac{3}{2} \ln(PV^{5/3}) - \frac{5}{2} \ln(N) + \Lambda \quad (7)$$

- The entropy of particles in a small region of phase space is conserved under Hamiltonian motion.
- $PV^{5/3}$ is conserved exactly only in cases where
 - Frozen-in-flux approximation is valid
 - Pressure is isotropic
 - Shape of energy dependence of distribution function is conserved in the drift
- Constraints on $PV^{5/3}$ are weaker and more complicated when one or more of these assumptions are violated.

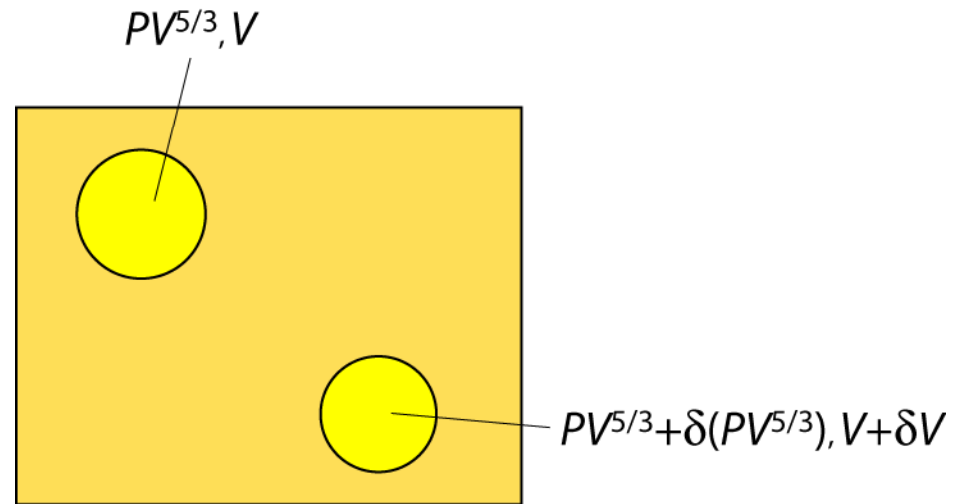
3. Interchange Instability

Interchange Instability Criterion – Ideal MHD, low β

- Standard textbook criterion for interchange instability (*Schmidt, Physics of High Temperature Plasmas*, 2nd ed., 1979):

- Exchange flux tubes with equal magnetic flux.
- Assuming adiabatic compression, potential energy decreases under the exchange if

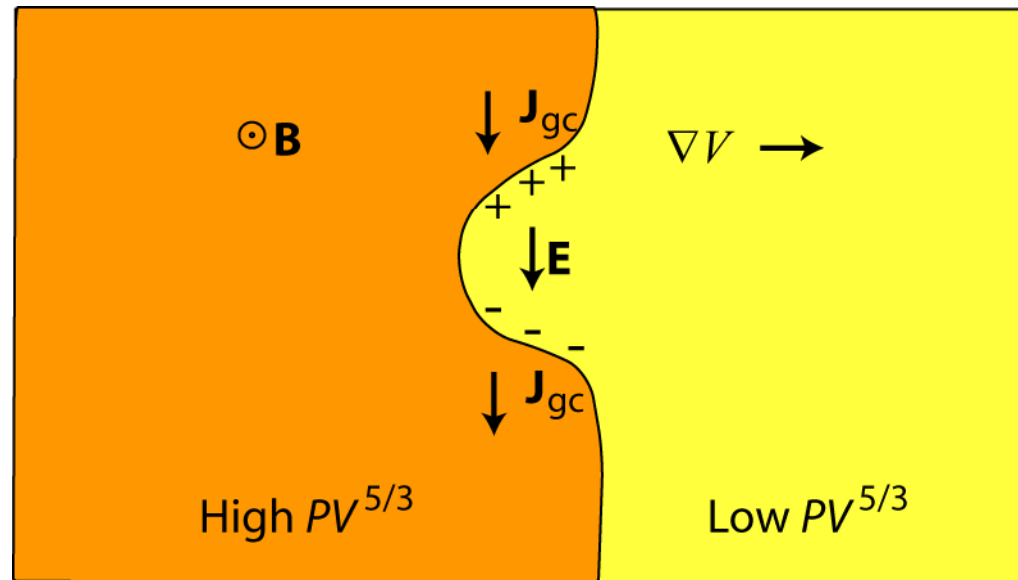
$$\delta(PV^{5/3})\delta V < 0$$



- This analysis assumes that the magnetic field does not vary in the interchange.
 - Just considers the change in particle thermal energy.
 - This simple interchange is most meaningful for a low- β plasma.

Intuitive Picture of Interchange Instability

$$\mathbf{v}_{GC} = \frac{\mathbf{B} \times \nabla(\lambda V^{-2/3})}{qB^2}$$



- Picture shows situation where higher- $PV^{5/3}$ flux tubes are nearer the Earth, on lower-volume flux tubes.
- The divergence of gradient/curvature-drift current produces charges on the sides of the ripple
 - Produces an E field that causes the ripple to grow → instability.
- The system is unstable if $PV^{5/3}$ decreases in the direction of increasing V . See *Xing and Wolf (JGR, 112, A12209, 2007)* for details.

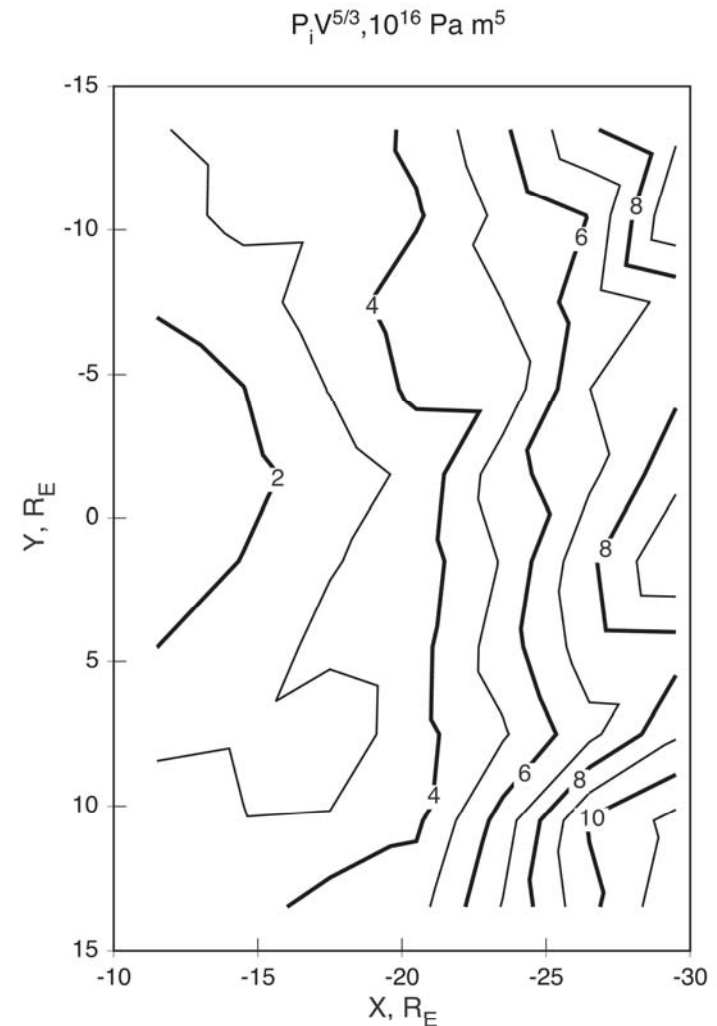
4. Statistical Plasma-Sheet Models and Pressure-Balance Inconsistency

Entropy in the Statistical Plasma Sheet

- *Borovsky et al. (JGR, 103, 20297, 1998)* showed that nV increases with geocentric distance and examined the mild increase of $P/n^{5/3}$ with distance.
- *Garner et al. (JGR, 108 (A8), 2003)* combined the T89 B-field model and *Paterson et al. (JGR, 103, 11811, 1998)* to make contour maps of equatorial $PV^{5/3}$.
- *Xing and Wolf (JGR, 112, 12209, 2007)* combined T96 B-field model with Tsyganenko-Mukai (*JGR, 108(A3), 2003*) plasma sheet to make contour maps of equatorial $PV^{5/3}$.
- *Kaufmann et al. (JGR, 114, A00D04, 2009)* obtained equatorial contour maps of $PV^{5/3}$ using Geotail data to obtain both pressures and magnetic fields.
- *Wang et al. (JGR, 114, A00D02, 2009)* computed partial entropies for different invariant energies λ and also used the statistical flow velocities to determine whether the partial entropy is constant along a drift path.

Pressure Balance Inconsistency

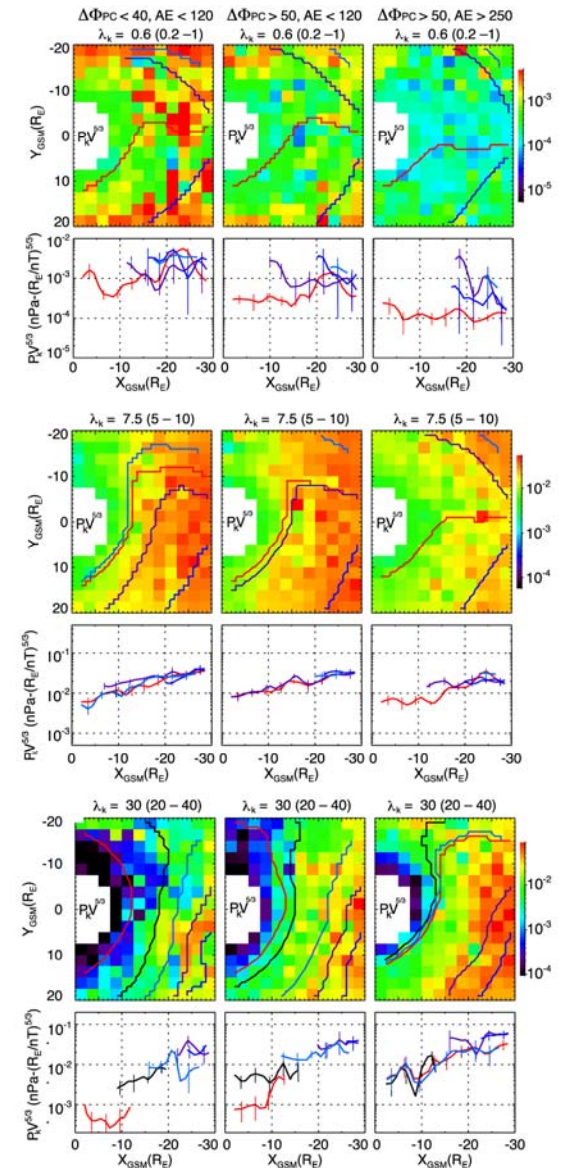
- All of these statistical analyses agree that entropy increases with geocentric distance, which is roughly the direction of $\nabla\Phi$.
- The inconsistency between the theoretical expectation that $PV^{5/3}$ should be roughly constant in the plasma sheet and the fact that $PV^{5/3}$ increases downtail in statistical models is called the “pressure balance inconsistency” or sometimes the “pressure crisis” (Erickson and Wolf, *GRL*, 897, 1980).
- “Entropy inconsistency” would have been a better name.
- $P/n^{5/3}$ is much more uniform than $PV^{5/3}$. It’s not that the flux tubes have gotten adiabatically cooled as they move earthward. They’ve lost particles (Borovsky, Kaufmann).



(Kaufmann et al., *JGR*, 109, A08204, 2004)

Conservation of Partial Entropy Along Drift Paths

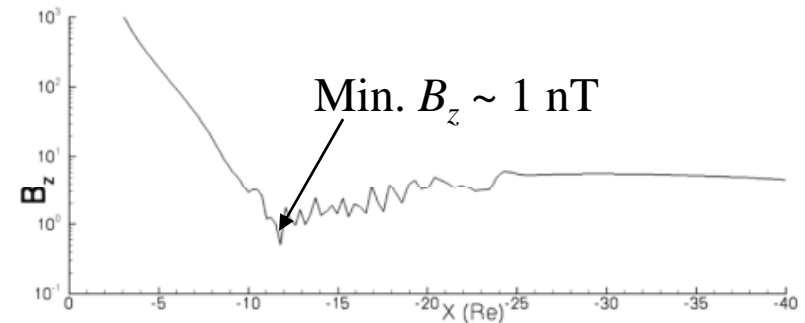
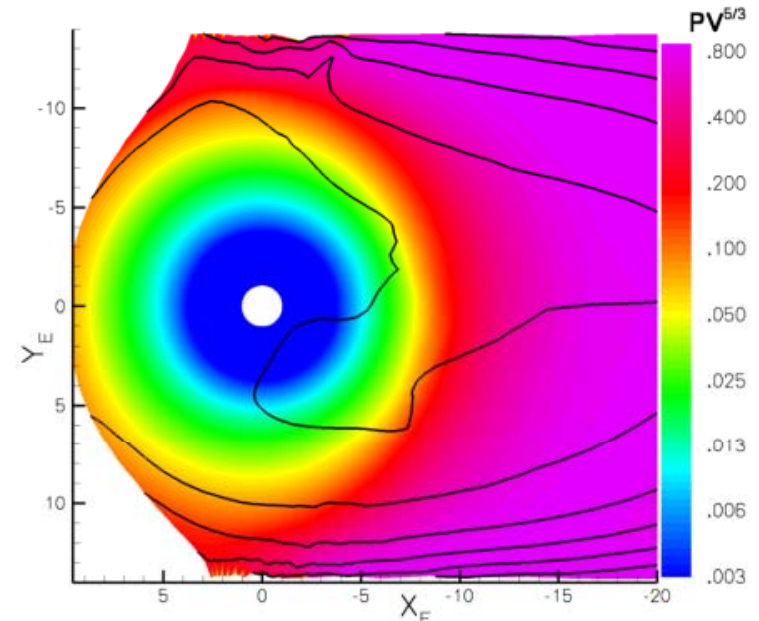
- Wang *et al.* (*JGR*, 114, A00D02, 2009) investigated the conservation of partial entropy (for given energy invariant λ_s), along drift paths, which were computed assuming electric fields estimated from the average flow velocities.
- The paper interprets the deviations from constancy of the partial entropy along drift paths as insignificant.



5. Entropy-Conserving Self-Consistent Solutions

Strong, Steady Adiabatic Convection

- When we enforce strong convection for hours in the RCM-E code, which keeps recalculating the magnetic field to keep it in approximate force balance with the RCM-computed $PV^{5/3}$ values, we always get a configuration that is highly stretched in the inner plasma sheet.
- $PV^{5/3}$ was assumed to be uniform on a boundary out in the tail.
- Note that $PV^{5/3}$ is nearly uniform beyond $\sim 10 R_E$, in contrast to statistical models.
- When we run RCM-E for a long time with a strong potential drop, the configuration reaches a highly stretched configuration
 - Nothing like a substorm expansion
 - No injection into the ring current

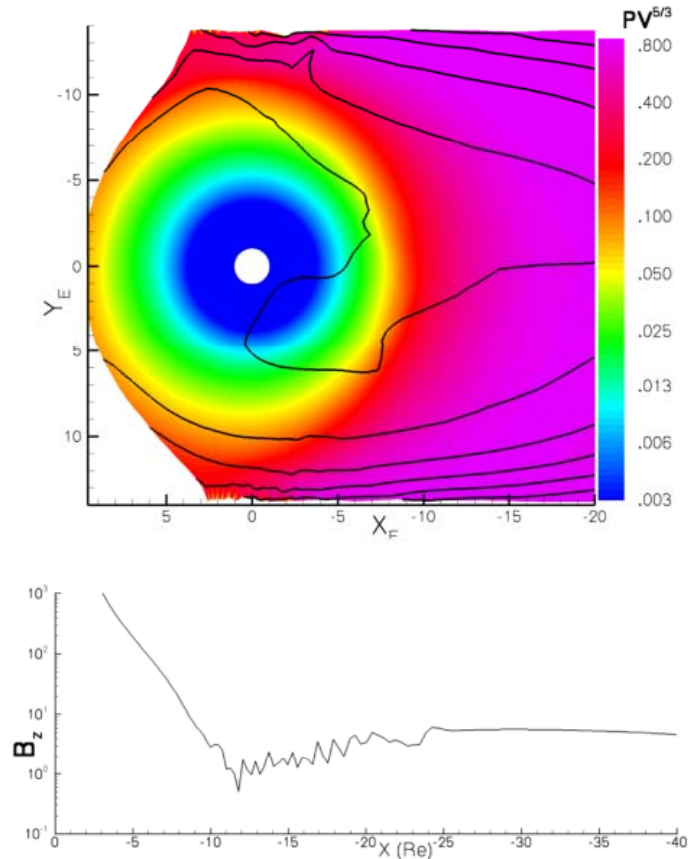


120 kV potential drop.

C. Lemon (Ph.D. thesis, Rice, 2005)

Pressure-Balance Inconsistency

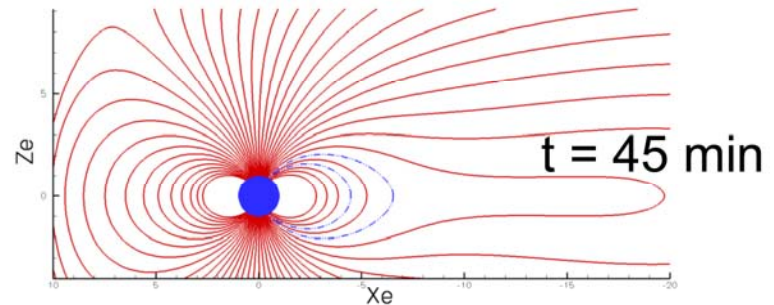
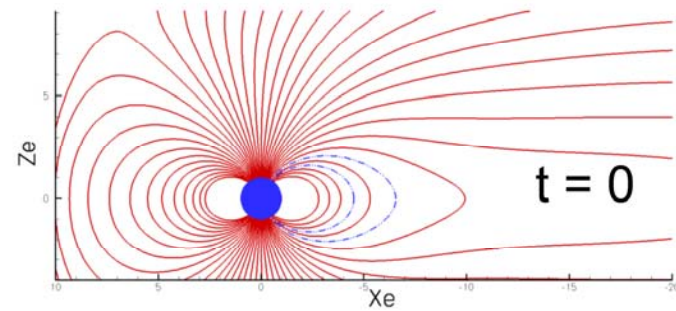
- The equatorial particle pressure decreases slowly downtail.
- In statistical models, the flux tube volume increases more rapidly.
- Thus $PV^{5/3}$ normally increases downtail.
- The RCM-E model avoids this in a steady convection configuration like the one shown to the right by creating a deep minimum in equatorial field strength in the inner plasma sheet (~ 1 nT). The inner plasma sheet flux tubes grow bigger, allowing volume to increase downtail only slowly.
- Qualitatively similar results: *Hau* (*JGR*, 96, 5591, 1991), *Erickson* (*JGR*, 97, 6505, 1992), *Toffoletto et al.* (*ICS-3 Proceedings*, 1996), *Lemon et al.* (*GRL*, 31, L21801, 2004), *Wang et al.* (*JGR*, 109, A12202, 2004).



(Lemon, Ph.D. thesis, Rice, 2005)

Connection to Substorm Growth Phase

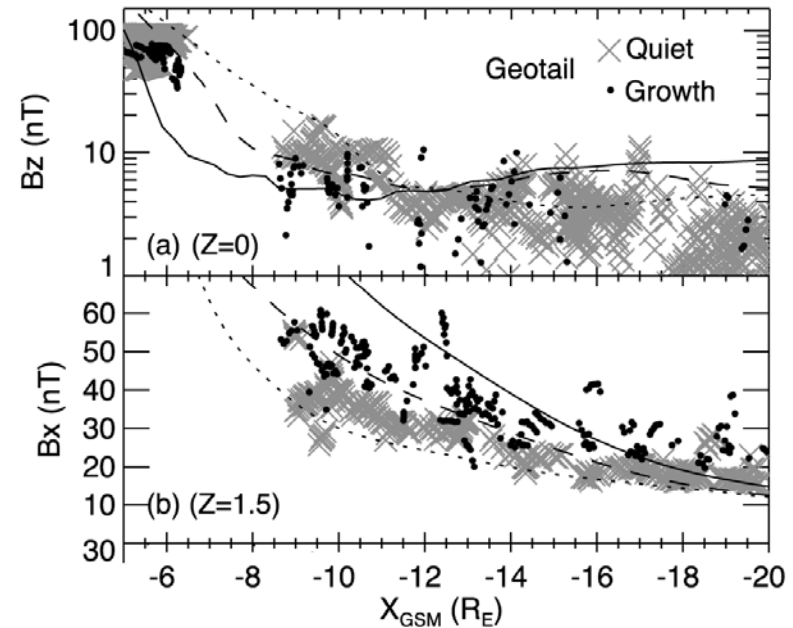
- Our group's interpretation of the highly stretched configuration is that steady adiabatic convection from out in the tail naturally produces a highly stretched inner plasma sheet.
 - Tail lobe field also strengthens.
 - Increased energy stored in the tail.
- Resembles a substorm growth phase.
- Natural interpretation is that, if the physical configuration gets stretched enough, then some instability gets triggered, which causes violation of the adiabatic condition and reduces entropy on some flux tubes
(*Toffoletto et al., Proc.ICS-5, 2000*)



(C. Lemon, Ph. D. thesis, Rice, 2005)

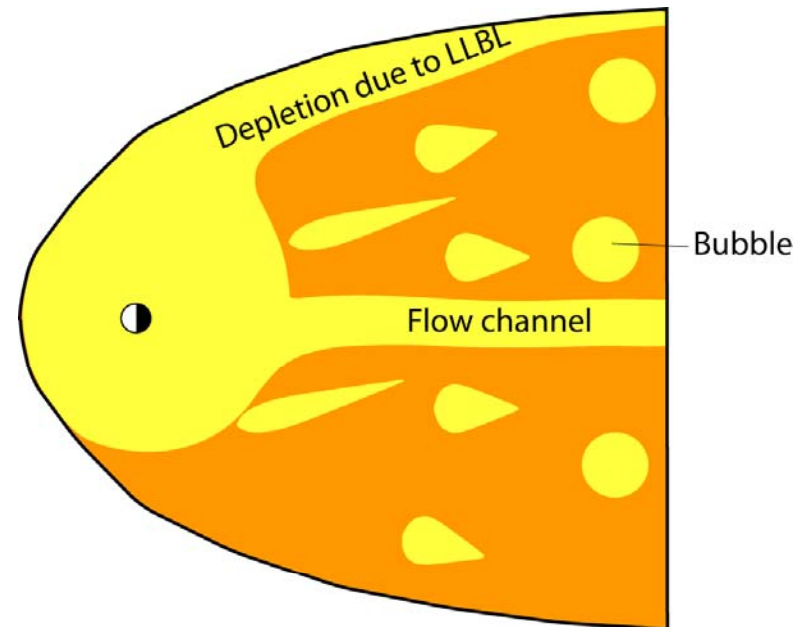
Different Calculation

- Using a somewhat similar procedure, *Wang et al. (JGR, 109, A12202, 2004)* get somewhat less stretched configurations.
 - They never get configurations as stretched as the one from *Lemon (2005)*.
- Differences in the *Wang* and *Lemon* calculations:
 - *Wang et al.* adopted a boundary condition with cool ions on the dusk side and allowed flow in through that boundary. *Lemon* enforced weak $E \times B$ drift out through the flanks.
 - While *Lemon* used a friction-code equilibrium solver to get a full 3D equilibrium, *Wang et al.* modified a T96 model to achieve equilibrium in the xz plane.
 - *Lemon* used an RCM-computed self-consistent potential electric field, while *Wang et al.* use an MSM-based assumed potential.
- *Wang* calculation still exhibits the pressure balance inconsistency, because its inner plasma sheet is more stretched than Tsyganenko models, but the stretching is not as extreme as in RCM-E calculation, and it agrees with growth-phase data.



Resolution of the Pressure Balance Inconsistency

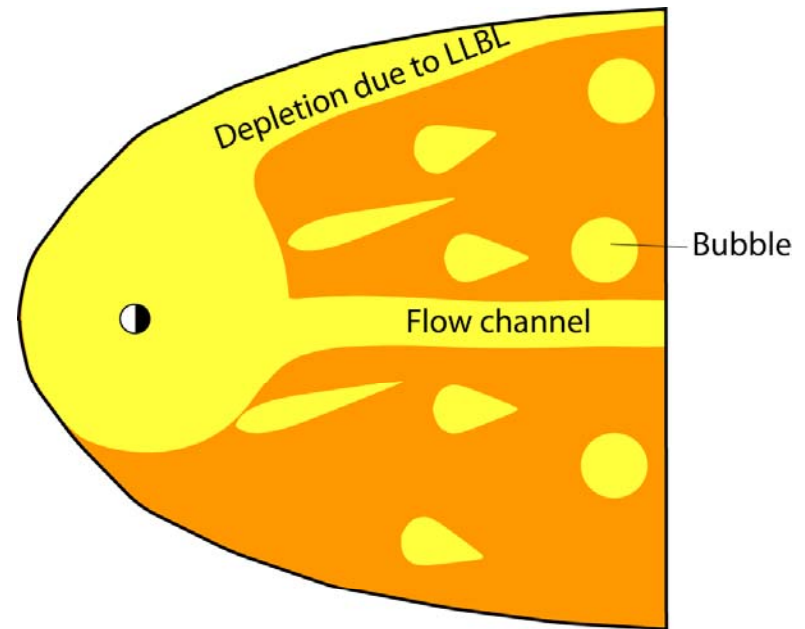
- Two main mechanisms have been suggested:
 1. Gradient/curvature drift. If the dawnside LLBL produces ion population with $PV^{5/3}$ much lower than in the distant tail, and a lot of the inner plasma sheet comes from the LLBL, then the inner plasma will have smaller $PV^{5/3}$ than the middle and distant sheet.
 - Development of idea: *Tsyganenko (Planet. Space Sci., 30, 1007, 1982), Kivelson and Spence (GRL, 15, 1541, 1988), Spence and Kivelson (JGR, 98, 15487, 1993), Wang et al. (GRL, 29 (24), 2002; JGR, 109, A12202, 2004; JGR, 114, A00D02, 2009), Lyons et al. (JGR, 114, A00D01, 2009).*
 - Works best for periods of slow convection.



Resolution of the Pressure Balance Inconsistency

2. Flow channels and bubbles with reduced $PV^{5/3}$ and strong earthward flow.

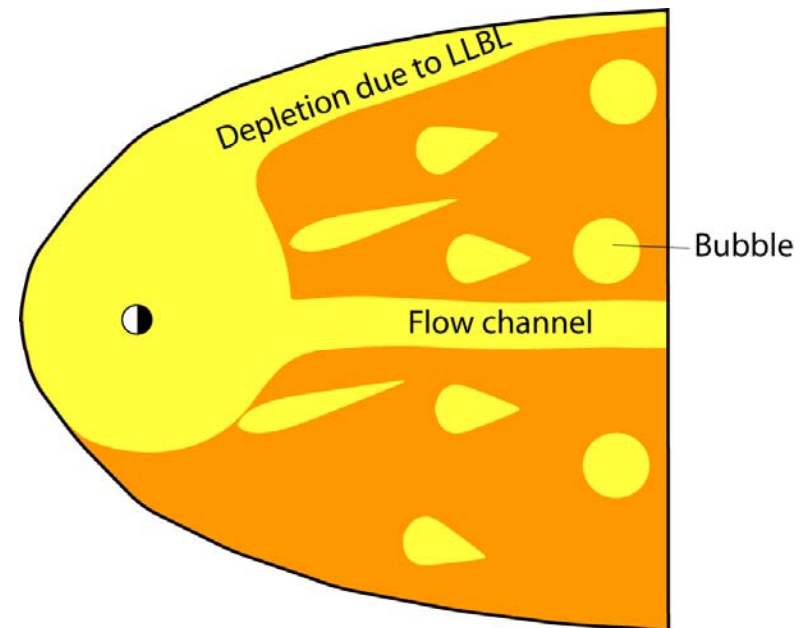
- Development of idea: *Sergeev and Lennartsson (PSS, 36, 353, 1988)*, *Sergeev et al. (PSS, 38, 355, 1990)*, *Pontius and Wolf (GRL, 17, 49, 1990)*, *Chen and Wolf (JGR, 98, 21409, 1993; JGR, 104, 14613, 1999)*.
- Both BBFs and substorm expansions produce bubbles.



- The bubbles and flow channels transport low- $PV^{5/3}$ flux tubes to the inner plasma sheet.
- If bubbles (BBFs) and flow channels, combined with the gradient/curvature-drift effect, provide enough low- $PV^{5/3}$ flux tubes to the inner plasma sheet that the magnetic field doesn't stretch to the breaking point, you get a Steady Magnetospheric Convection event.
 - If they don't, then you get a substorm expansion.

Resolution of the Pressure Balance Inconsistency

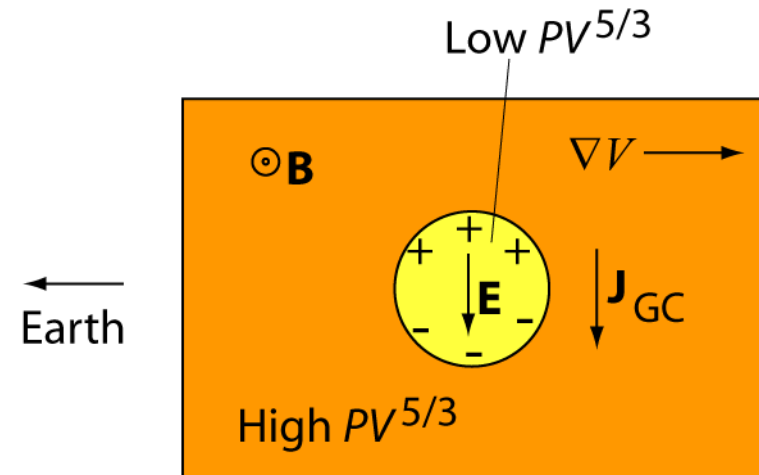
- Both gradient/curvature-drift and bubble mechanisms operate.
- They are not mutually exclusive.
 - In fact, the combination should be stronger than the sum of its parts.
 - If a large fraction of the total transport is in flow channels, bubbles, then the electric field across the orange (high- $PV^{5/3}$, slow flow) channels decreases, which makes gradient/curvature drift a more efficient loss mechanism.
- There is evidence of flow channels coming in from flanks, where V and thus $PV^{5/3}$ are small (*Perroomian, Lu*)
 - We need to simulate cases like that.



6. Bubbles in the Plasma Sheet and Creation Mechanisms

Bubbles in the Plasma Sheet

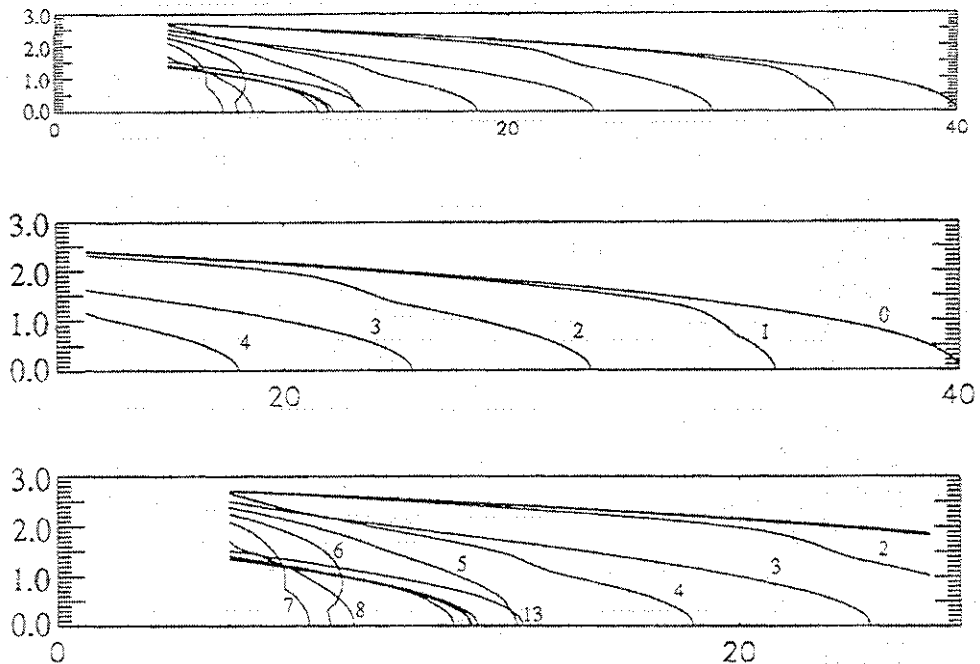
- *Pontius and Wolf (GRL, 17, 49, 1990)* pointed out that a plasma-sheet “bubble”, a flux tube that has lower $PV^{5/3}$ than its neighbors, will move earthward, toward the direction of smaller flux tube volume.
 - Analogous to the upward motion of a bubble in a liquid.



- A blob, which is a flux tube with $PV^{5/3}$ higher than its neighbors, moves out from Earth.
- *Chen and Wolf (JGR, 98, 21409, 1993)* suggested that bursty bulk flows were bubbles.
- *Chen and Wolf (JGR, 104, 14613, 1999)* developed a theory of bubble dynamics, visualizing a bubble as a thin ideal-MHD filament.
 - Finite conductance earthward boundary.

Motion of Thin-Filament Bubble

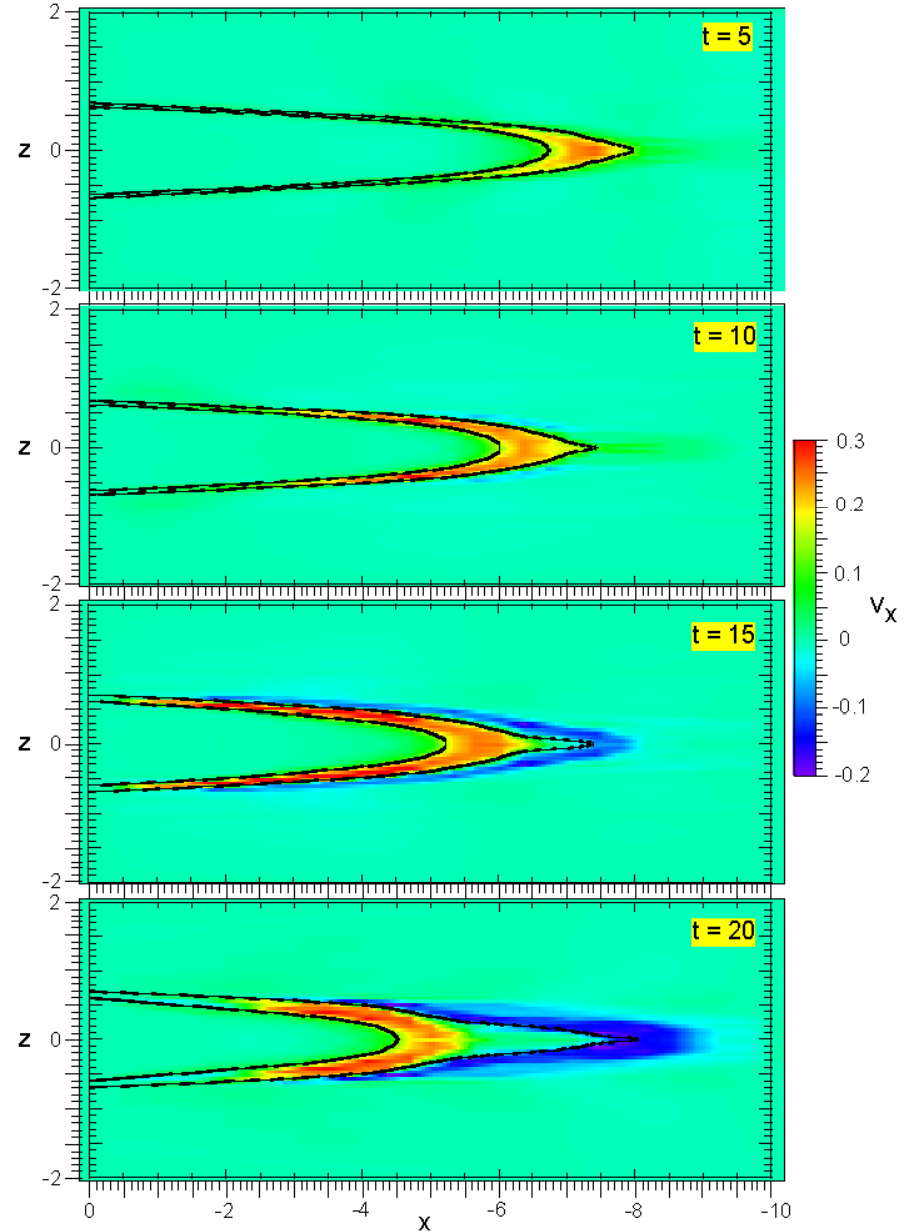
- Field line shortens.
- Second and third panels zoom in on tailward and earthward regions.
- An Alfvén wave and a slow mode propagate earthward.
- When the Alfvén wave hits the conducting left boundary (ionosphere), that end of filament starts to move equatorward.
- Filament overshoots equilibrium position but eventually settles into equilibrium.
- Simulation was ideal-MHD with some friction between filament and background.



From *Chen and Wolf (1999)*.
Numbers represent minutes.

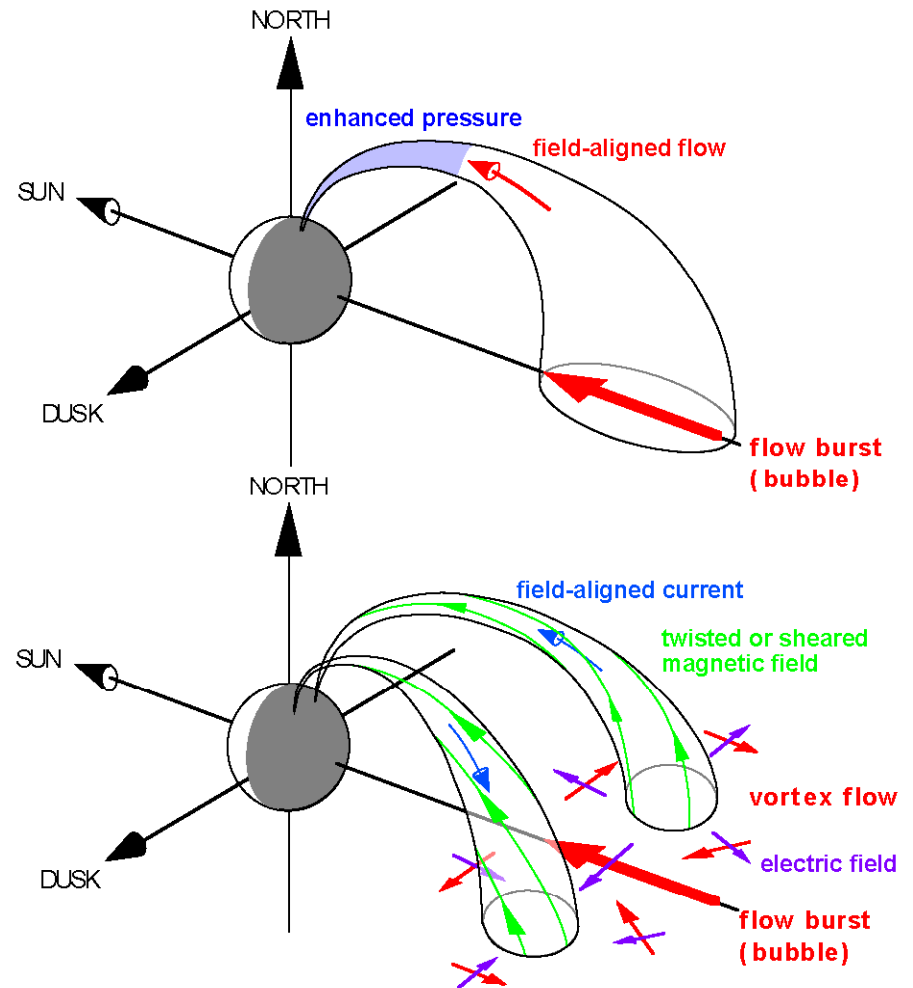
3D MHD Simulation of a Bubble

- *Birn et al. (Ann. Geophys., 22, 1773, 2004)* did a full 3D MHD simulation of a bubble.
- In the plot, colors show sunward velocities V_x .
- Black lines are magnetic field lines.
- These calculations have a perfectly conducting earthward boundary.



Bubble Geometry

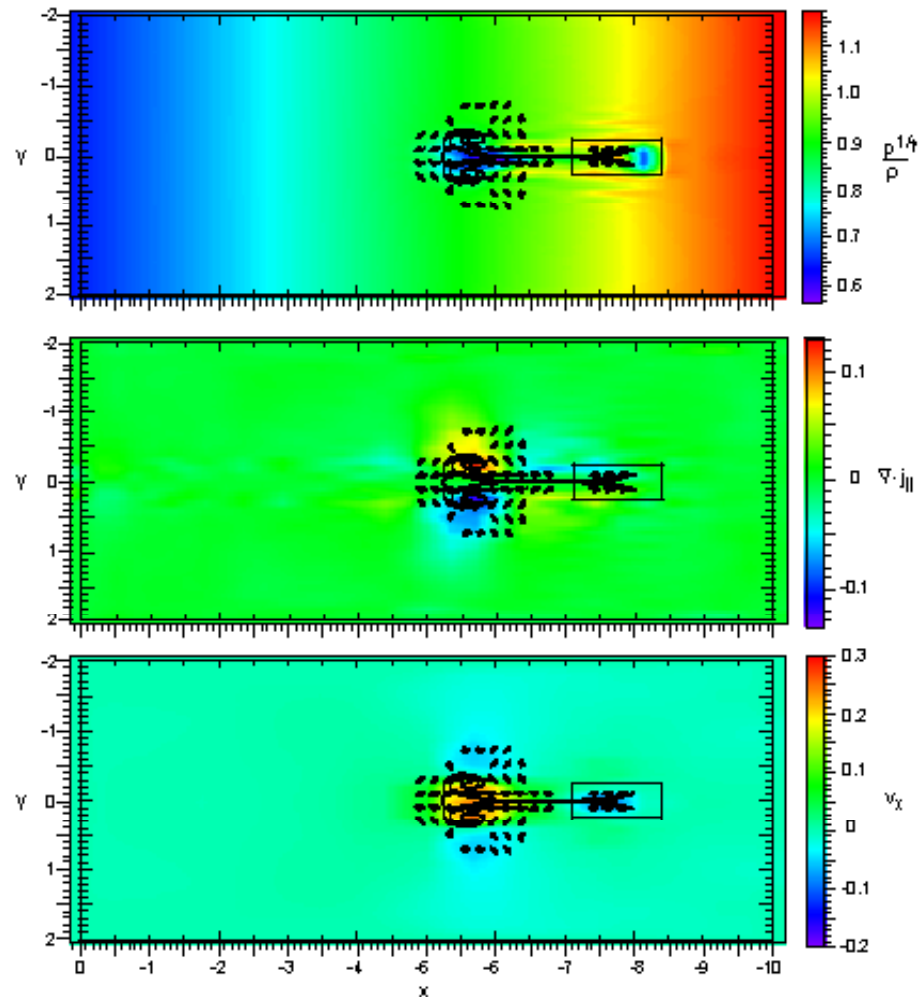
- Flux tubes have to get out of the way of the earthward moving bubble.
 - Creates a twin-vortex flow



From *Birn et al.*
(*Ann. Geophys.*, 22, 1773, 2004)

Shape of Bubble in xy -Plane

- Ambient flux tubes ahead of the bubble are deflected to the sides and then fill in the wake.
- Chen-Wolf (1999) thin-filament simulations represent the central part of the bubble.
 - Don't deal with shape
- In 3D MHD calculations, the details of the shape in xy plane depend on numerical viscosity.



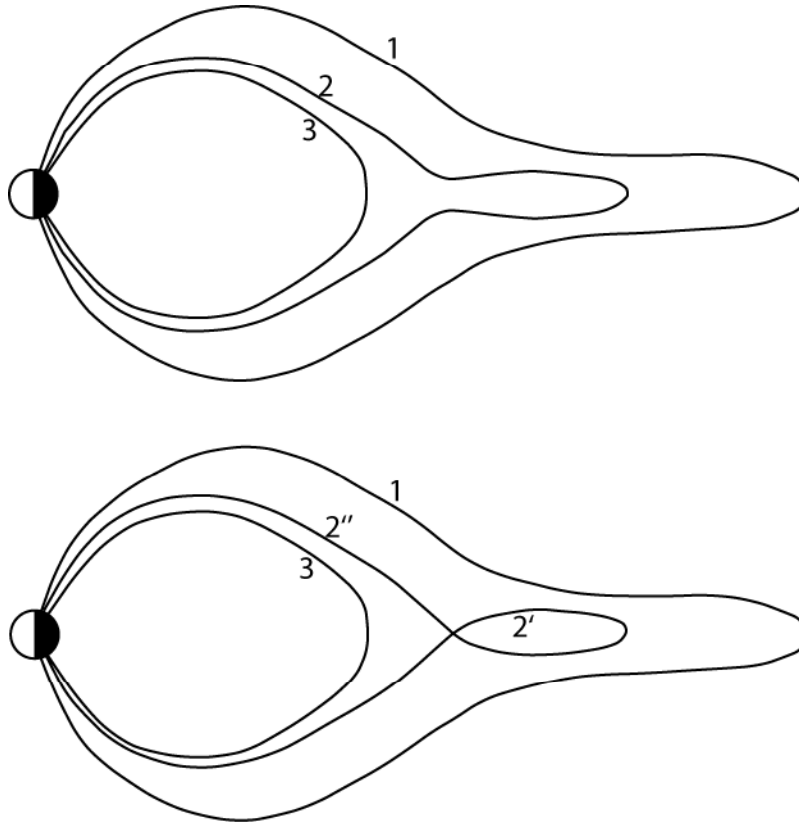
Birn et al. (2004)

Some Bubbles Observed in the Plasma Sheet and in Auroral Streamers

- *Sergeev et al. (JGR, 101, 10817, 1996) (ISEE)*
- *Lyons et al. (JGR, 108 (A12), 2003) (Geotail)*
- *Apatenkov et al. (Ann. Geophys., 25, 801, 2007) (Cluster)*
- *Kauristie et al. (JGR, 105, 10677, 2000) (Wind)*
- *Nakamura et al. (JGR, 23, 553, 2005) (Cluster)*
- *Sergeev et al. (Ann. Geophys., 22, 537, 2004). (DMSP, Polar UVI)*

- Most of these are bursty bulk flows, although one is a substorm.

Reconnection as a Source of Bubbles



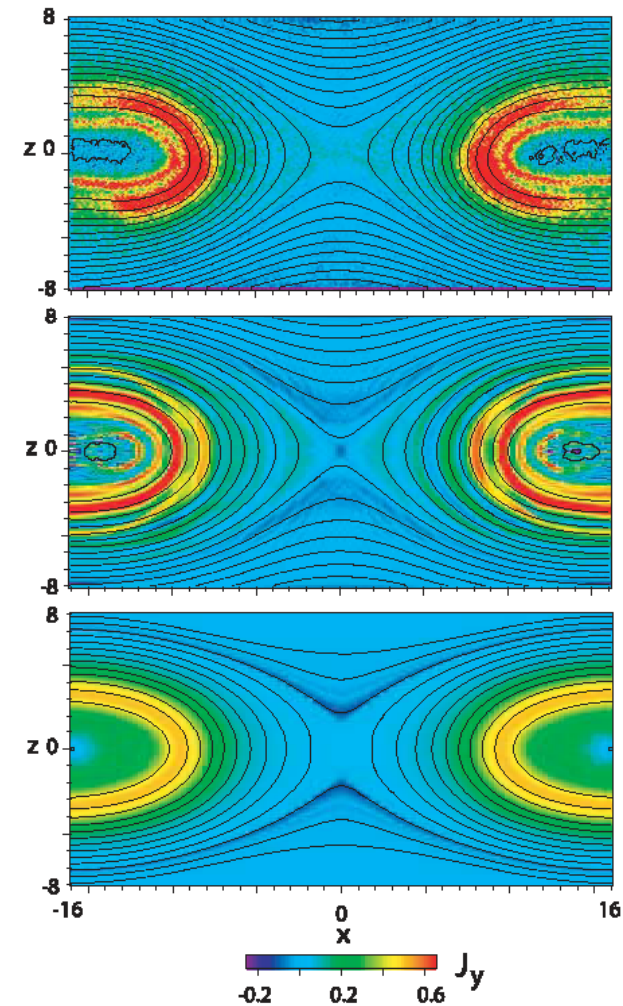
- Suppose reconnection occurs on flux tube 2, splitting it into 2' and 2''.
- In the ideal-MHD approximation, entropy is conserved and

$$P_{2'}^{3/5} V_{2'} + P_{2''}^{3/5} V_{2''} = P_2^{3/5} V_2$$

- But of course reconnection can't occur in ideal MHD.
 - Can entropy still be approximately conserved in a more realistic treatment that allows reconnection?

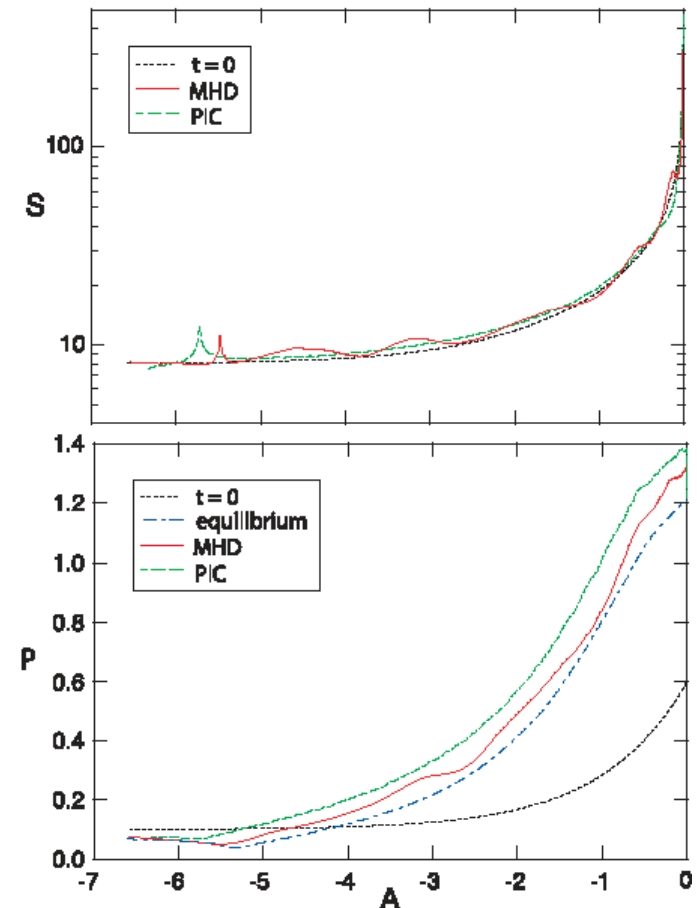
Entropy Conservation in Reconnection

- *Birn et al. (Phys. Plasmas, 13, 092117, 2006)* looked at entropy conservation in a simulation of the “Newton Challenge”, which represented reconnection in a Harris-sheet idealized situation.
- The plot shows final state in PIC simulation (top), MHD simulation (middle), and minimum energy configuration for the same entropy function.



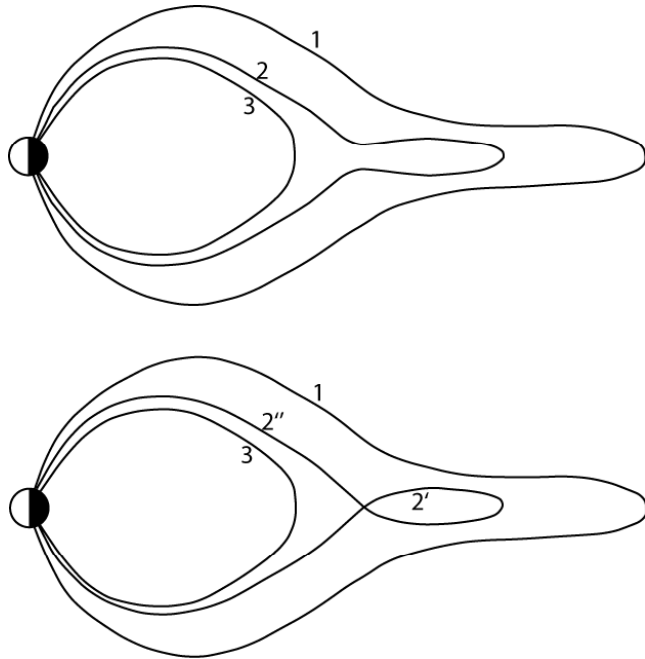
Entropy Conservation in Reconnection

- The upper plot looks at $S=P^{3/5}V$ as a function of flux-function A , which labels field lines, comparing initial S with values after reconnection had occurred.
- PIC and MHD values both differ little from the initial entropies, even though the pressure changed a lot.
- Entropy was approximately conserved on nearly all flux tubes.
- Birn showed similar simulations at this meeting that included a guide field (B_y). Entropy still conserved pretty well.



Birn et al. (JGR, 114, A00D03, 2009)

How Does Closed-Field-Line $PV^{5/3}$ Change in Reconnection?



- Consider thin flux tube centered on line 2.
- The conclusion from Birn's work is that we should expect

$$P_{2'}^{3/5}V_{2'} + P_{2''}^{3/5}V_{2''} \approx P_2^{3/5}V_2$$

so that

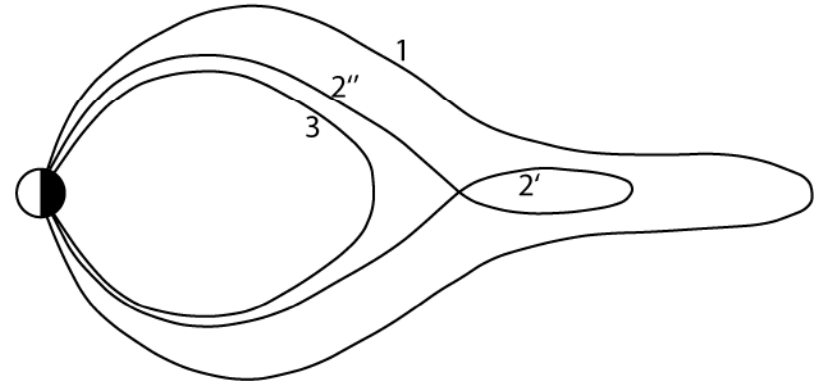
$$P_{2''}V_{2''}^{5/3} < P_2V_2^{5/3}$$

which means that the new closed flux tube (2'') has lower entropy than the old one (2).

- Therefore, reconnection creates a bubble.
- Standard reconnection theory applies: plasma exits the reconnection area at \sim Alfvén speed.
- $PV^{5/3}$ is a crucial boundary condition for RCM.
- Identification of the outflow as a bubble helps you visualize what happens to the ejecta in its interaction with the high-flow region near the Earth.
- For mathematical model of a reconnection process that produces a bubble, see
 - *Sitnov et al. (GRL 32, L16103, 2005)* (2D equilibrium solution)
 - *Sitnov et al. (GRL, 34, L15101, 2007)* (kinetic theory solution)

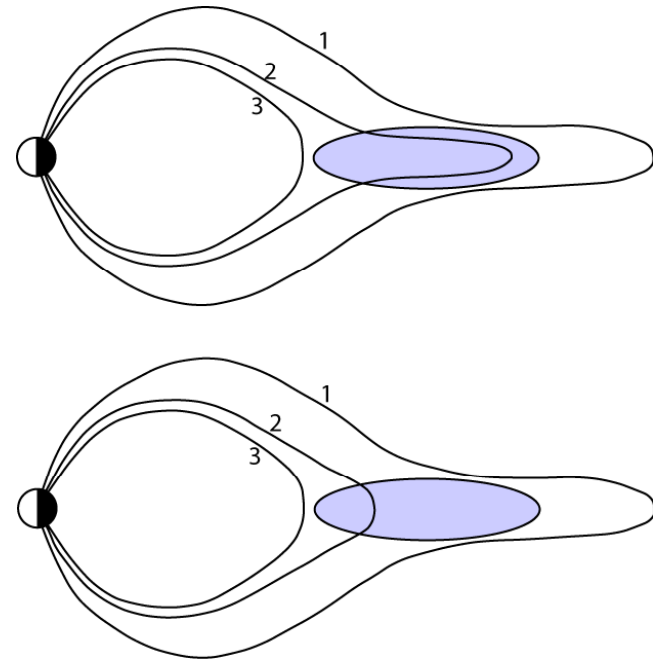
Effect of a Guide Field on the Plasmoid

- A substantial B_y can make what looks like a plasmoid in 2D into a closed-field-line structure that crosses a section of the plasma sheet as a flux rope.
- This structure has a very large flux tube volume, which makes it a “blob” of high entropy $PV^{5/3}$.
 - It will move antisunward, which is what a plasmoid would do.

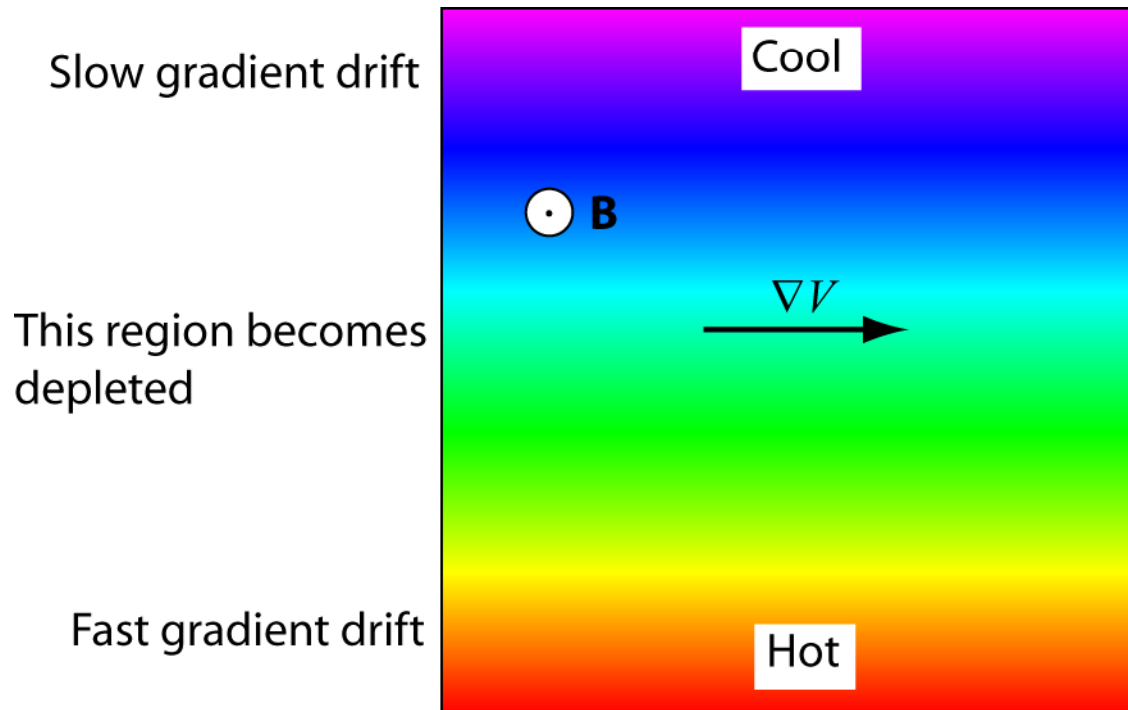


Could Tail-Current Disruption Create a Bubble?

- Suppose tail-current disruption (*Lui et al, JGR, 97, 1461, 1992*) happens in the shaded area, and a positive E_y appears there, the result of anomalous resistivity (or whatever) in the region of positive J_y .
- Now consider flux tube bounded by 1 and 2, and another bounded by 2 and 3.
- Then field line 2 will $E \times B$ drift earthward, and equatorial B_z will increase between lines 2 and 3.
- The volume of the tube bounded by 2 and 3 will decrease, creating an earthward-moving low-entropy bubble.
- The volume of the tube bounded by 1 and 2 will increase, creating a tailward-moving high-entropy blob.
- Between the earthward-moving bubble and the tailward-moving blob, the plasma sheet should thin, possibly creating an X-line.

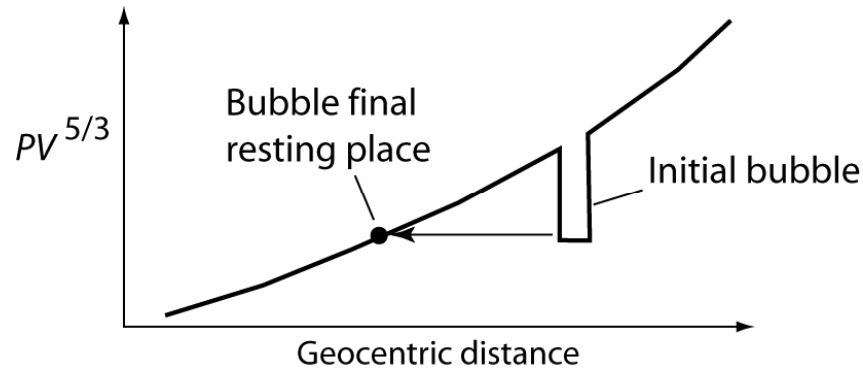


Lyons Mechanism for Reducing $PV^{5/3}$



7. Restrictions on Bubbles That can Reach the Inner Magnetosphere

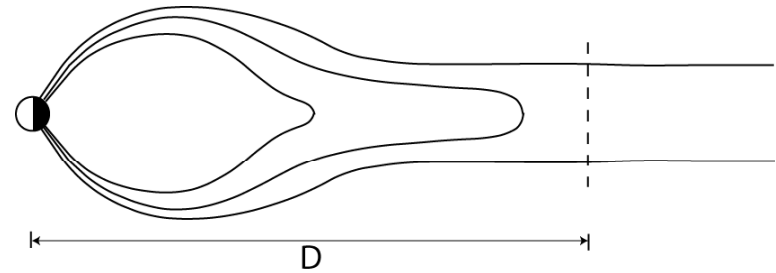
A Bubble's Final Resting Place



- If reconnection in the distant tail creates a bubble that has, say, half the $PV^{5/3}$ that the original closed flux tube had, that bubble will move earthward but probably won't penetrate into geosynchronous orbit.
 - If mixing between bubble and background is negligible, the bubble will move earthward only until it finds a location where the background $PV^{5/3}$ matches its own.
 - Transfer between background and bubble reduces the distance of travel.
- This earthward motion of bubbles helps to resolve the pressure balance inconsistency.

Constraints on Injectable Flux Tubes in Reconnection Picture

- RCM-E simulations [*Lemon et al.*, 2004] suggest that flux tubes with $PV^{5/3} > \sim 0.08 \text{ nPa} (R_E/nT)^{5/3}$ cannot assume quasi-dipolar form and enter inner magnetosphere.
 - This tentative conclusion needs more analysis and sensitivity study.
- When an X-line occurs at a distance D downtail, the *Birn et al.* [2006] result suggests that the entropy on the post-reconnection closed flux tube is equal to the entropy on the part of the pre-reconnection flux tube that lies within D of the Earth.
- If reconnection occurs at distance D downtail, and entropy is conserved except near the reconnection site, then only a limited number of closed flux tubes near the lobes will have small enough entropy to be capable of transport to the inner magnetosphere.
 - Reconnection of tail-lobe field lines should produce bubbles of very low entropy.



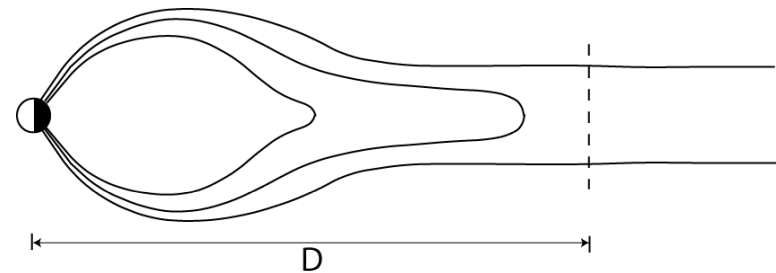
Constraints on Injectable Flux Tubes in Reconnection Picture

- In analyzing storms, one could estimate entropy-related quantities like $\int d\Phi PV^{5/3}$ or $\int d\Phi P^{3/5}V$ (*) for the storm-time ring current, where $d\Phi$ is an element of magnetic flux, given the fact that the similar integral

$$\frac{3}{2} \int PVd\Phi \quad (\dagger)$$

is the particle energy in the ring current.

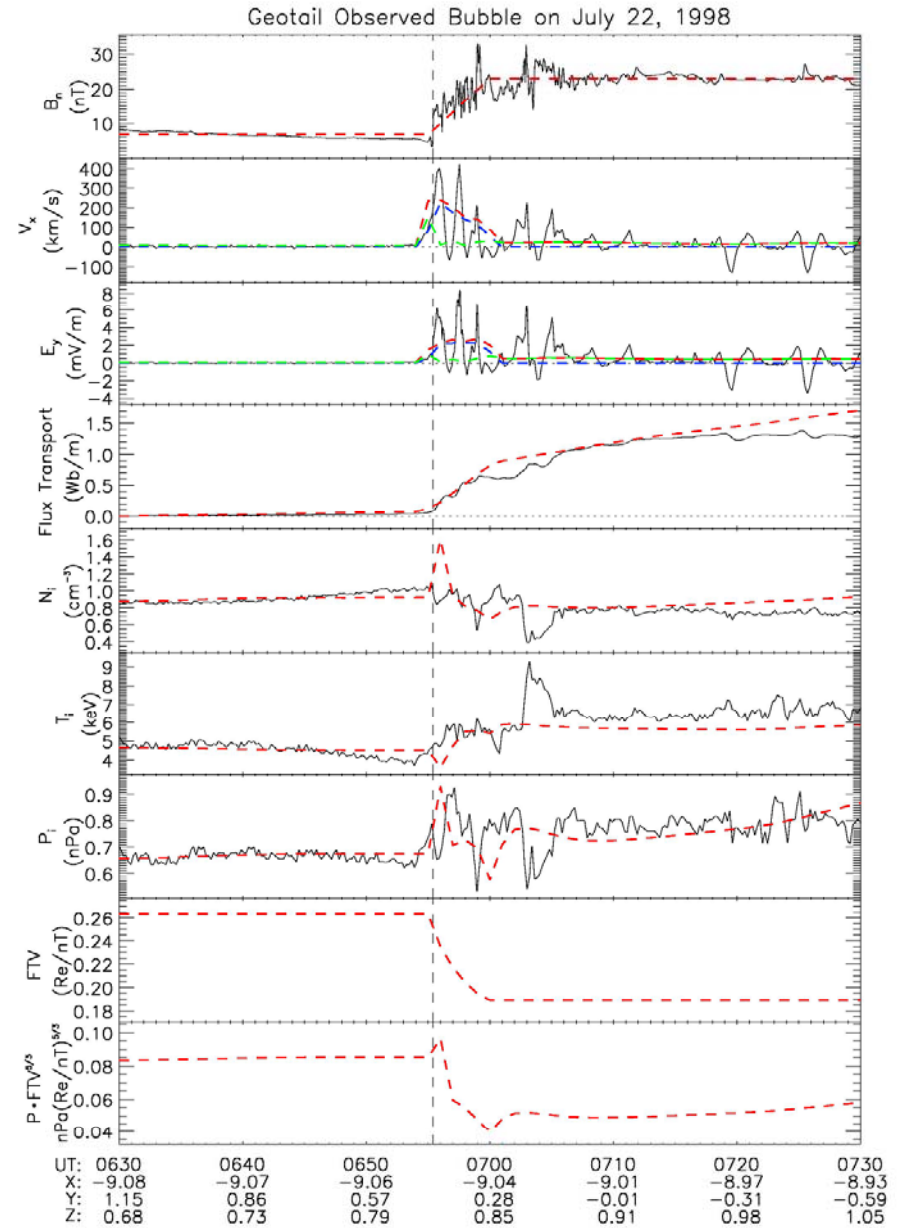
- For a given event, if you can estimate one of the integrals in (*) for an assumed model of how reduced-entropy flux tubes are created in the tail, you can compare it with (\dagger) to see whether the mechanism is strong enough.
- A very rough analysis of this type was carried out by *Kan et al. (JGR, 112, A04216, 2007)*



8. RCM Simulation of a Bubble in a Substorm

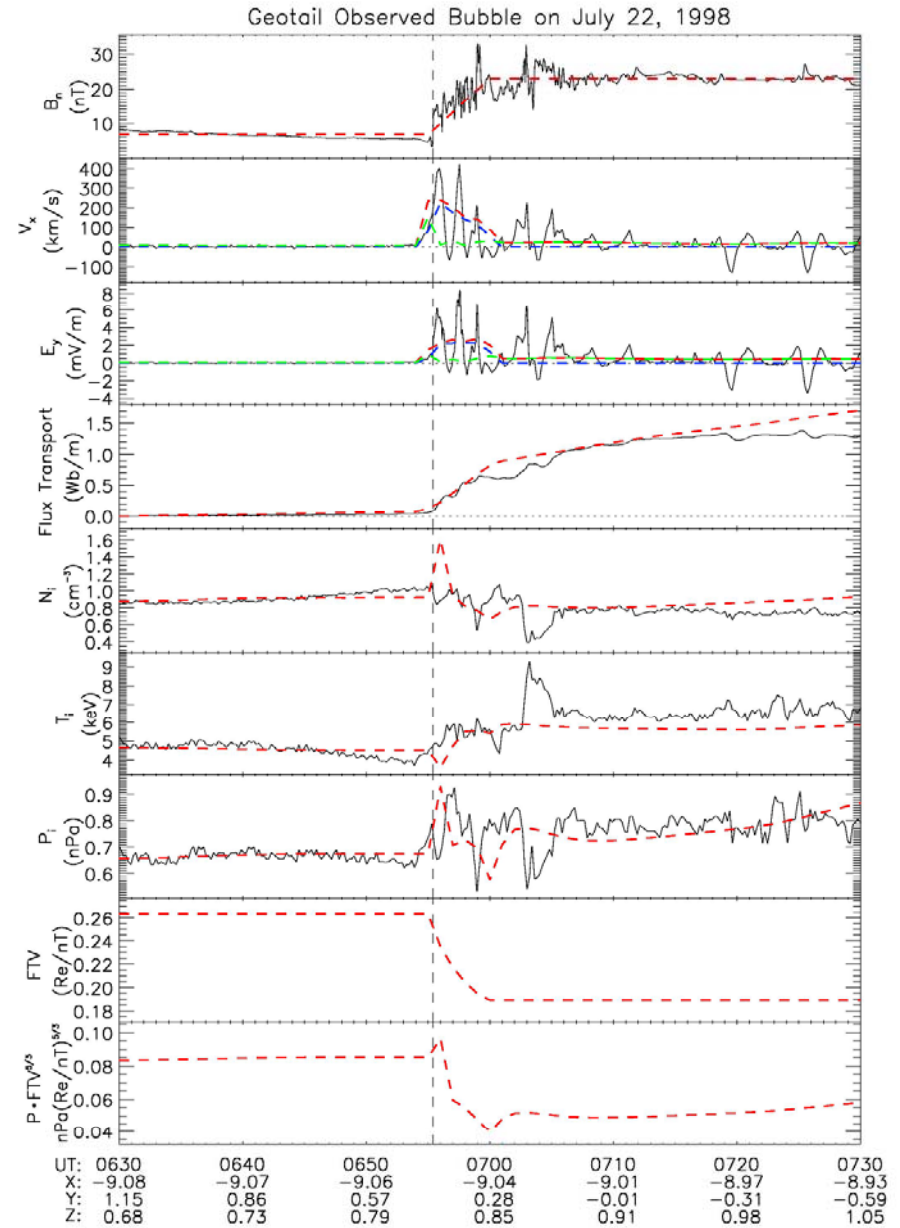
RCM Simulation of 7/22/98 Substorm

- Geotail data from $X \approx -9$, $Y \approx 0$.
- Top panel, which displays B_z , shows extreme stretching, followed by dipolarization starting at about 0655 UT.
- Second panel shows earthward velocity, which becomes basically positive starting about 0654 UT.
- Third panel shows E_y calculated from plasma data.
- Fourth panel shows $\int E_y dt$, which is the amount of magnetic flux transported earthward, per unit y .



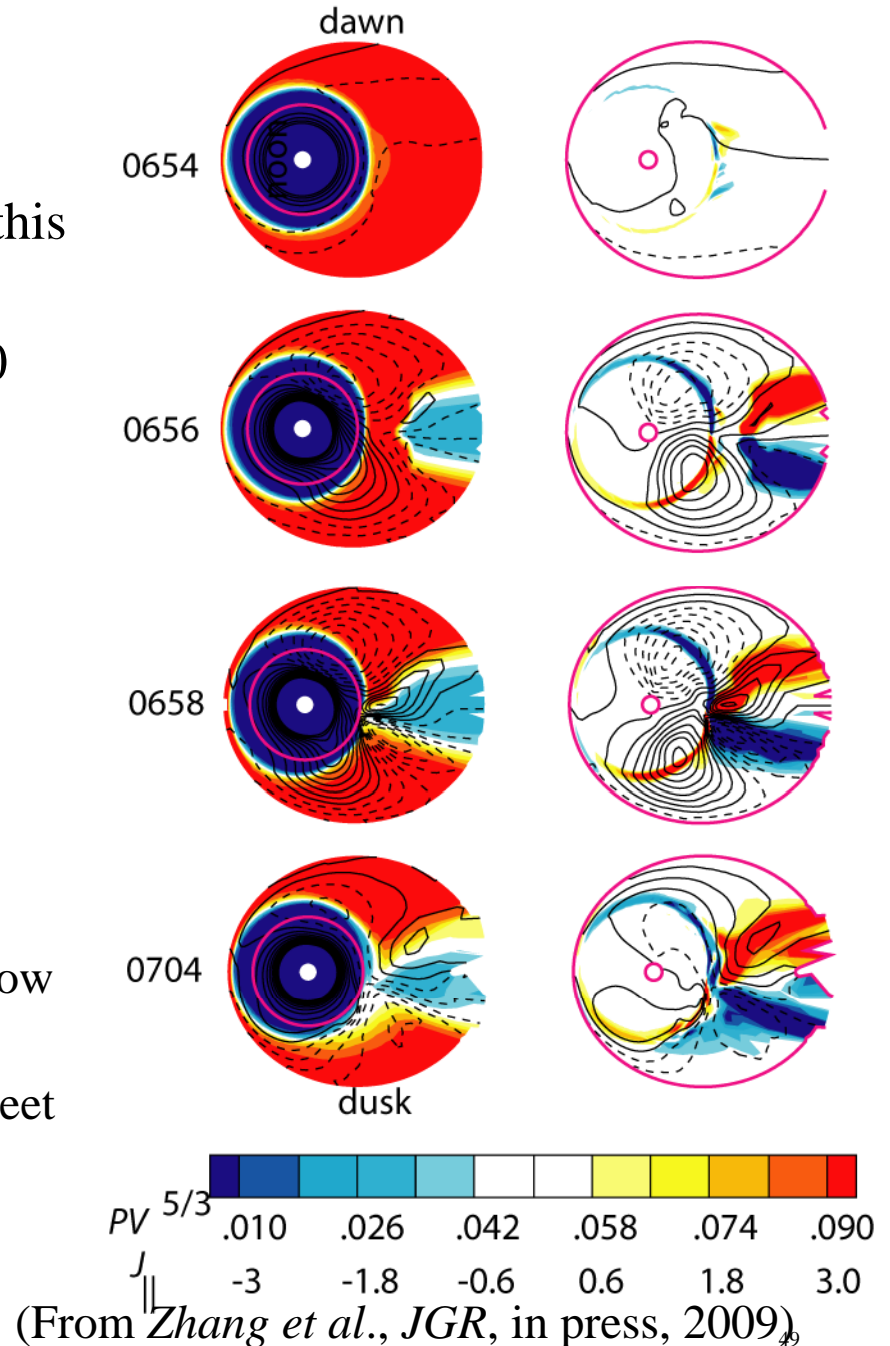
RCM Simulation of 7/22/98 Substorm

- Black curves are Geotail data.
- Dashed red curves are RCM-computed values.
- We adjusted RCM inputs to agree with Geotail, particularly the degree of dipolarization and the correct $\int E_y dt$.
- The last two panels show V and $PV^{5/3}$ estimated from the Geotail data, using the method of *Wolfe et al. (JGR, 101, A12218, 2006)*.
- Note that estimated $PV^{5/3}$ drops significantly in the dipolarization, indicating a bubble.



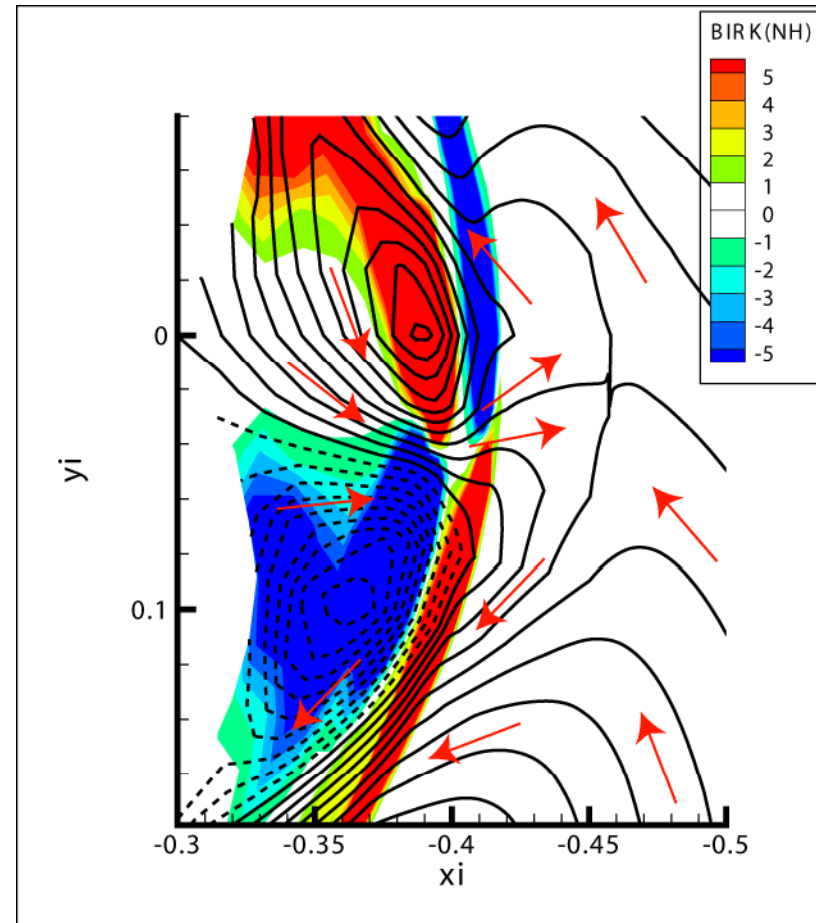
Sample Simulation Result

- We have looked at many features of this brief event. An example:
- Dipolarization occurs at $t=0655-0700$
- Left column shows $PV^{5/3}$ (color) and trajectories for average plasma sheet ion.
 - Blue area is the bubble.
- Right column shows downward Birkeland current and ionospheric equipotentials mapped to equatorial plane.
 - Region-1 sense Birkeland currents flow on the sides of the bubble.
 - Region-2 current flows on plasma sheet inner edge.



Another Sample Result

- View of computed ionospheric equipotentials and Birkeland current in the ionosphere. The Sun is to the left and $y_i=0$ is local midnight.
- The bubble is moving equatorward (to the right).
- Eastward and westward flow on the eastern and westward sides of the bubble represent plasma getting out of the way of the bubble.

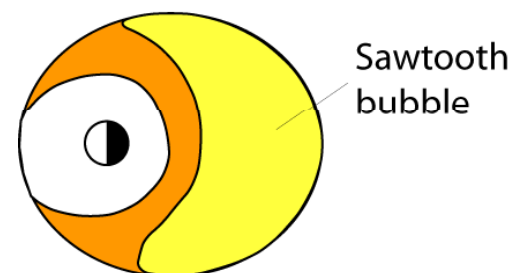
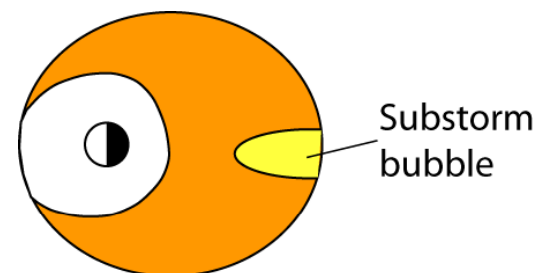


(From Zhang *et al.*, *JGR*, in press, 2009)

9. RCM-E Simulation of a Sawtooth Event

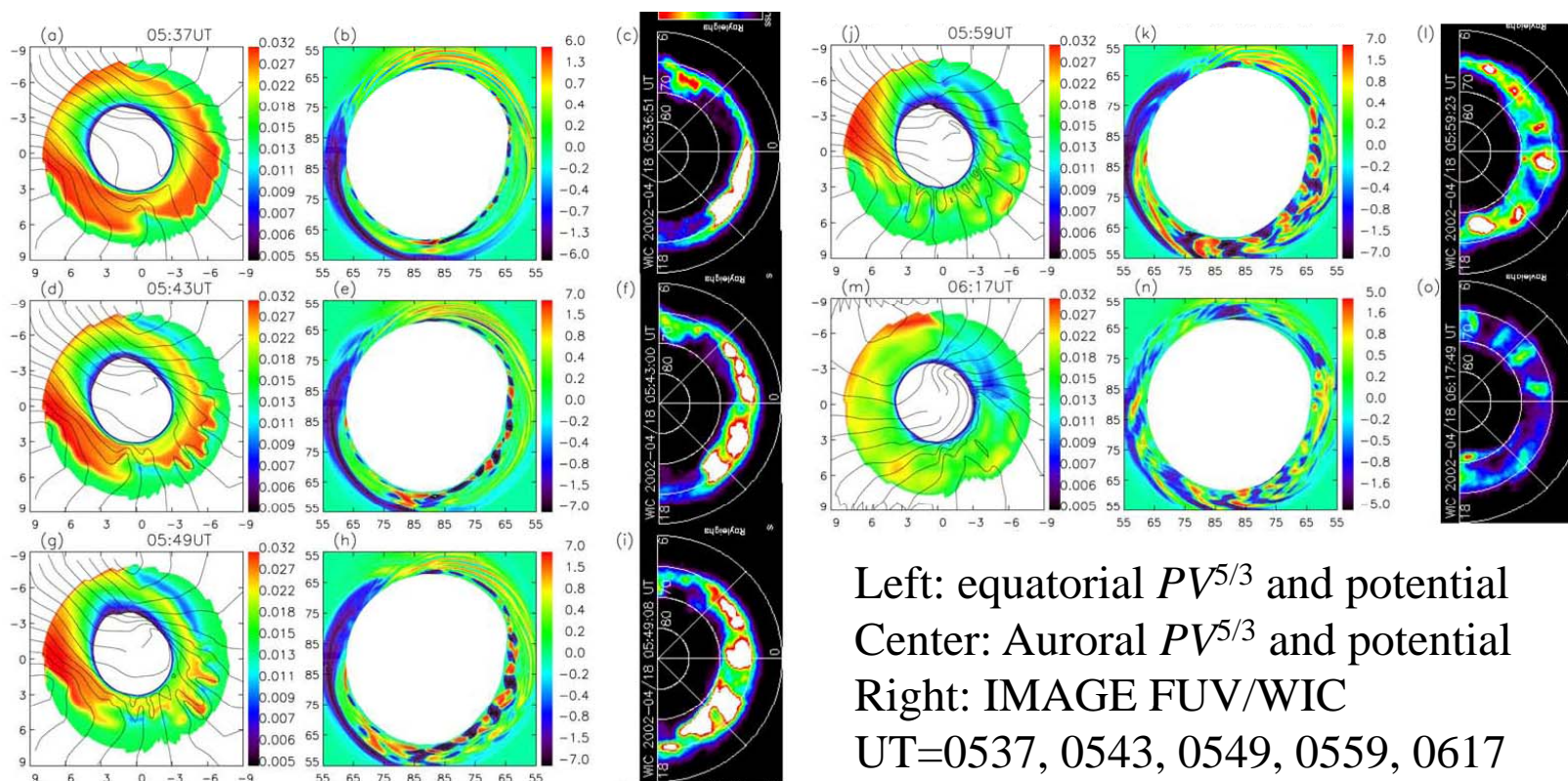
The Difference Between Sawtooth Events and Substorms

- The early part of a substorm expansion phase covers a narrow range of local time and thus involves a narrow bubble.
- A sawtooth event involves nearly simultaneous dipolarization over a wide range of LT.
 - The dipolarization can only happen if $PV^{5/3}$ decreases.



- The leading edge of any bubble tends to be interchange unstable, since there $PV^{5/3}$ decreases in the direction of increasing V .
- In the substorm case, the bubble moves rapidly earthward, so the interchange instability at the leading edge doesn't have much time to develop.
- In the sawtooth case, interchange instability develops along the leading edge.

RCM-E Simulation and Auroral Images



- In the 0530 sawtooth, flux tubes of low entropy (green/blue) enter RCM region.
- Interchange instability develops, with outreaching high-entropy fingers (red/orange) and Birkeland currents on the sides of the fingers.
- IMAGE FUV saw series of north-south aligned auroral structures, which we tentatively interpret as resulting from interchange fingers.

Summary

- $PV^{5/3}$ is conserved in the plasma sheet under certain restrictive conditions.
- Steady-state adiabatic-convection solutions exist for the plasma sheet, but their inner regions are much more stressed than statistical models.
- Pressure-balance inconsistency is apparently resolved by processes that break the adiabatic condition in the plasma sheet and by transport of bubbles in from boundary layers.
- Reconnection, current disruption, and differential gradient/curvature drift all break conservation of $PV^{5/3}$ and should be capable of producing bubbles.
- A bubble comes to rest when its $PV^{5/3}$ is the same as its neighbors.
- A bubble entering the inner magnetosphere injects fresh particles and produces characteristic disruptions of the normal E field and current patterns.
- A sawtooth event, which is a very wide bubble, naturally generates interchange fingers.
- The overall conclusion is that bubbles play an important role in plasma sheet transport and dynamics.

Backup Slides

Approaches

- Construct a series of magnetic-field models for the event that are designed to be consistent with measurements during the event.
 - This is the approach used by *Kubyshkina et al.* (*JGR*, 107 (A6), 2002; *JGR*, 113, A08211, 2008).
 - This is probably the most accurate approach but involves a lot of work.
- We designed a simple little algorithm that estimates V and $PV^{5/3}$ near a measuring spacecraft, using just measurements made by the spacecraft.

Estimation of $PV^{5/3}$ from Single-Spacecraft Measurements

- $PV^{5/3}$ plays a vital role in plasma-sheet transport, but nobody has figured out a way to measure it.
- Average values can be estimated from statistical models of the plasma and magnetic field
 - But that doesn't help in figuring out the changes in $PV^{5/3}$ that occur during an injection event.
- We have made an initial effort at developing a formula for estimating $PV^{5/3}$ locally from measurements on a single spacecraft.
- Start from a simple analytic model of force-balanced tail:

$$A(x, z) = -A_o \cos\left(\frac{\pi z}{2\Delta}\right) e^{-\alpha x} \quad P(A) = \frac{A^2}{2\mu_o} \left[\left(\frac{\pi}{2\Delta}\right)^2 - \alpha^2 \right]$$
$$V(A) = \frac{\pi}{\alpha \sqrt{B_z(A)^2 + 2\mu_o P(A)}}$$

Estimation of V and $PV^{5/3}$ from Single Spacecraft Measurements

- These 2D analytic expressions, which don't include a representation of the effect of the Earth, don't represent the real inner plasma sheet very well.
- To account for this in a highly approximate way, we replace α by a flexible function of parameters B_z and $(x^2+y^2)^{1/2}$, which can be measured by a spacecraft at the center of the current sheet:

$$V_E(x, y) = \frac{10^C \left(\sqrt{x^2 + y^2} \right)^D \left(B_{zE}(x, y) \right)^F}{\sqrt{B_{zE}(x, y)^2 + 800\pi P_E(x, y)}}$$

Estimation of V and $PV^{5/3}$ from Single Spacecraft Measurements

$$V_E(x, y) = \frac{10^C \left(\sqrt{x^2 + y^2} \right)^D \left(B_{zE}(x, y) \right)^F}{\sqrt{B_{zE}(x, y)^2 + 800\pi P_E(x, y)}}$$

- Algorithms for estimating P_E and B_{zE} from measurements off the equatorial plane:

$$\log_{10} [P_E(x, y, z)] = \log_{10} \left[P(x, y, z) + \frac{B_r(x, y, z)^2}{2\mu_0} \right] - G \frac{B_r(x, y, z)}{B_z(x, y, z)}$$

$$B_{zE}(x, y, z) = B_z(x, y, z) \sqrt{1 + \frac{B_r(x, y, z)^2}{B_z(x, y, z)^2 + 2\mu_0 P(x, y, z)}}$$

- Fitting to 18 *Tsyganenko* (1996) models for a range of conditions leads to the following choices of adjustable parameters:

$$C = 0.7368, D = 0.7634, F = -0.3059, G = 0.0107$$

for magnetic fields in nT, pressure in nPa, flux tube volume in R_E/nT .

Testing of First-Try Algorithm

- Testing has to be done with models, because nobody has figured out a way to measure flux tube volume.
- T89 models.
 - RMS error in $\log_{10}(V) \sim 0.09$, in $\log_{10}(PV^{5/3}) \sim 0.16$.
- Friction code equilibrium model with a depleted channel.
 - Algorithm gave good agreement with this model, which was very different from the Tsyganenko models to which the model was tuned.
- Full MHD thin-filament calculations (*Chen and Wolf, 1999*) that include high-speeds.
 - The formula underlying our estimation algorithm came from assuming equilibrium, with $P = \text{constant}$ along magnetic field line, so there is no reason to expect good performance for times of fast flow.
 - Algorithm underestimates the final value of $PV^{5/3}$ by factor ~ 2 when observed Mach number > 0.2 .
- For details, see *Wolf et al. (JGR, 2006)*.
- We are still working on more tests and improvements.